G-rich Oligonucleotide Inhibits the Binding of a Nuclear Protein to the Ki-*ras* Promoter and Strongly Reduces Cell Growth in Human Carcinoma Pancreatic Cells†

Susanna Cogoi, Franco Quadrifoglio, and Luigi E. Xodo*

Department of Biomedical Science and Technology, School of Medicine, University of Udine, Piazzale Kolbe, 4, 33100 Udine, Italy

Received September 29, 2003; Revised Manuscript Received December 17, 2003

ABSTRACT: Oligonucleotides are able to recognize both nucleic acids and proteins with a high degree of specificity and are therefore investigated as a new and innovative class of therapeutic anticancer drugs. In the present study, we have constructed from Panc-1 cells a stable transfectant (AG transfectant) generating constitutively a short transcript (T-22AG), which is potentially capable of forming a triplex with a critical polypurine/polypyrimidine (*pur*/*pyr*) motif located in the Ki-*ras* promoter. Because of the presence of a G-rich element in its sequence, transcript T-22AG was also capable, under physiological conditions, of adopting a tetraplex conformation. We found that the levels of Ki-*ras* mRNA and $p21^{RAS}$ protein in the AG transfectant were, respectively, 52 ± 8 and 40 ± 4% of those observed in the control cell lines: untransfected Panc-1 cells and stably transfected Panc-1 cells producing a control transcript (T-22SCR). The downregulation of Ki-*ras* resulted in a strong reduction of colony formation (42 ± 7% of the control) and cell proliferation (34 ± 5% of the control) capacity. As in vitro experiments showed that the G-rich element of T-22AG (22AG) formed with the Ki-*ras pur*/*pyr* motif a triplex of low thermodynamic stability, it is unlikely that the strong bioactivity exhibited by transcript T-22AG is mediated by a triplex-based mechanism, although we cannot totally exclude that in vivo polyamine levels may increase the triplex stability. We found that 22AG adopted a tetraplex conformation and competitively inhibited the binding of a nuclear factor to the Ki-*ras pur*/*pyr* sequence. This effect was specific and virtually entirely abrogated when 22AG was denatured by heating. Our data showed that transcript T-22AG acted as a molecular aptamer, binding specifically to a nuclear factor essential for Ki-*ras* expression. The biological implications of this study are discussed.

Pancreatic carcinomas normally arise in the cells of the exocrine pancreas that are involved in the production of the digestive juices. These tumors are rather aggressive and show a profound resistance to extant treatments (*1*). The prognosis associated to pancreatic cancer is poor and reflects the current lack of effective treatment available and the urgent need of new therapeutic strategies in this area. The first genetic change detected in the majority (>90%) of pancreatic carcinomas are mutations in the Ki-*ras* gene (*2*). The Ki-*ras* gene is present in chromosome 12, locus 12p12.1, and regulates the growth and differentiation of many cell types (*3*). Ki-*ras* encodes a 21-kDa Ras protein, $p21^{RAS}$, which is located on the inner surface of the plasma membrane and acts as a molecular switch that transmits to the nucleus signals for cell proliferation (*4*). Protein $p21^{RAS}$ is in the active form when bound to GTP and in the inactive state when GTP is hydrolyzed to GDP. Point mutations at codon 12, 13, and 61 of Ki-*ras* impair the ability of $p21^{RAS}$ to hydrolyze GTP into GDP, so that the protein is maintained locked into the active state. Moreover, mutated Ki-*ras* is frequently found in many other human tumors, such as colorectal carcinomas, lung carcinomas, and myeloid leukaemia (*5*). In addition to activation by point mutations, the Ki-*ras* gene has been found amplified or overexpressed in some cancers (*6*−*8*). Studies conducted on transgenic mice showed that the presence of mutant Ki-*ras* allele is necessary for both the initiation of the tumorigenesis and for maintenance of the transformed state (*9*). So, it is now widely accepted that the Ki-*ras* gene represents an important molecular target in therapeutic strategies designed to inhibit the hyperproliferation of pancreatic tumor cells (*10*). Several molecular approaches have been developed pointing to reducing the altered Ki-*ras* gene product or eliminating its biological function. Antisense oligonucleotides have been used in three pancreatic cell lines with the major types of Ki-*ras* point mutations and were found to significantly reduce cell growth (*11*, *12*). Ribozymes designed to cleave specifically the mutated form of the Ki-*ras* mRNA, the GUU motif in codon 12, were found to reduce both the proliferation and colony formation in pancreatic tumor cells (*13*). Oligonucleotides forming antiparallel triplexes with the Ki-*ras pur*/*pyr*[1] motif have been used to inhibit the expression of murine Ki-*ras* (*14*, *15*). A 15mer peptide nucleic acid conjugated to the nuclear localization signal peptide and complementary to codon 12 in the mutated allele was found to significantly reduce cell growth in pancreatic carcinoma Panc-1 cells (*16*). Farnesyl transferase inhibitors of p21 (ras) farnesylation have been designed to prevent ras processing and induce cancer cell death (*17*). In this context, we pursue a new molecular strategy to downregulate the expression of

† This work was supported by PRIN 2001, CNR (CNRC00845_002 and FVG (3887, LR 3/1998).

* To whom correspondence should be addressed: Dr. Luigi E. Xodo, Department of Biomedical Science and Technology, School of Medicine, P.le Kolbe 4, 33100 Udine, Italy. Tel.: +39.0432.494395. Fax: +39.0432.494301. E-mail: lxodo@makek.dstb.uniud.it.

10.1021/bi035754f CCC: $27.50
Published on Web 02/13/2004

the Ki-*ras* gene in tumor cells. We focused our attention on a polypurine/polypyrimidine (*pur*/*pyr*) motif located in the gene promoter, 13 helical turns from transcription initiation. Previous studies on chromatin structure showed that this *pur*/*pyr* motif is sensitive to endogenous nuclease and S1 nuclease in supercoiled plasmids (*18*). Nuclease hypersensitive *pur*/*pyr* motifs are present in several oncogene promoters and seem to be associated with the non-B-form of DNA (*19*, *20*). It has been demonstrated that a *pur*/*pyr* motif present in the c-*myc* promoter, which is similar to that present in Ki-*ras*, can be engaged into a slow duplex/tetraplex equilibrium, which is thought to play a role in gene regulation (*19*, *20*). In addition to its potential capacity to extrude a tetraplex structure, the Ki-*ras pur*/*pyr* motif can form a triple-stranded DNA with G-rich oligonucleotides, under physiological pH (*21*−*23*). These oligonucleotides recognize the major-groove of the *pur*/*pyr* motif and form a local triple structure that can interfere with the promoter activity (*14*, *15*, *24*−*26*). With these premises, we constructed from Panc-1 cells, a transfectant cell line stably expressing a short transcript. This endogenously generated transcript harbored a 22mer G-rich element identical, but with opposite polarity, to the purine strand of the Ki-*ras pur*/*pyr* motif. This G-rich element could in principle form a local triplex with the Ki-*ras pur*/*pyr* motif or, alternatively, self-associate into a tetraplex (*19*, *20*). We found that the endogenously generated transcript caused a significant reduction of the levels of Ki-*ras* mRNA and protein $p21^{RAS}$, resulting in a dramatic decrease of proliferation and colony formation in the genetically modified Panc-1 cells. The 22mer G-rich element of transcript T-22AG formed a triplex of low stability with the Ki-*ras pur*/*pyr* target. Nonetheless, T-22AG exhibited a strong and specific antiproliferative effect in the transfectant cells. We interestingly found that 22AG inhibited in a sequence-specific manner the interaction between a nuclear factor and the Ki-*ras pur*/*pyr* motif. Polypurine 22AG recognized the nuclear protein through its unusual structure which appeared to be a tetraplex. However, despite both 22AG and scramble 22SCR were found to form tetraplex structures, only the former was associated with biological activity. Taken together, these data suggest a new molecular strategy for the design of molecules to selectively interfere with the proliferation in pancreatic carcinoma cells. The sequestration of the nuclear factor recognizing the Ki-*ras pur*/*pyr* motif by a tetraplex-forming oligonucleotide seem to be a highly attractive approach.

MATERIALS AND METHODS

Plasmid Construction. Plasmid mU6 was kindly supplied by Sarah B. Noonberg (University of San Francisco). mU6 was derived from plasmid pGem1 and contained promoter and termination sequences from the human small nuclear U6 gene. It contained two unique restriction sites, *XhoI* and *NsiI*, that allow the insertion of a DNA fragment of any sequence. We inserted in mU6 the duplexes obtained by annealing (i) 5′-TCGAGGAGGGGGAGAAGGGAGAAGGGATGCA and 5′-TCCCTTCTCCCTTCTCCCCCTCC to obtain an expression vector (pU6−CT) generating a 76mer AG-motif transcript (T-22AG); and (ii) 5′-TCGAGAAGAGAAGAGAAGAAGAGAAGATGCA and 5′-TCTTCTCTTCTTCTCTTCTTCTTC to obtain vector pU6−RN generating a 76mer random-sequence AG-motif transcript (T-22SCR) to be used as control.

Cell Cultures and Stable Transfectants. Human exocrine pancreas epithelioid carcinoma cells (*27*), Panc-1, were purchased from the Istituto Zooprofilattico Sperimentale of Brescia (Italy). The cells were cultured in DMEM medium, containing 100 U/mL penicillin, 100 μg/mL streptomycin, 200 mM L-glutamine, and 10% foetal bovine serum (Celbio, Milano, Italy). Cells were maintained in logarithmic phase of growth subculturing them twice a week. The stable transfectants were obtained as follows. Panc-1 cells were seeded at a concentration of 2.4×10^5/mL in 100-mm diameter Petri dishes and grown in 10 mL of medium. After 24 h, the cells were cotransfected with 15 μg of pU6−CT or 15 μg of pU6−RN and 1.5 μg of pCDNA3, bearing the resistance to genetycin (G418). Forty-eight-hours post transfection, 700 μg/mL of G418 were added to the medium and selection was maintained for 3 weeks. Single colonies were isolated and grown separately. Total RNA extracted from these cells was analyzed for the production of the expected transcripts by Northern blot.

RNA Isolation and Northern Blotting. Total RNA was isolated from the stable transfectants (5×10^6 cells) following a standard guanidinium thiocyanate−phenol−chloroform extraction. About 10 μg of total RNA extract was run in a 2% agarose denaturing gel, blotted on a positively charged nylon membrane (Pall Gelman Sciences, MI) by capillarity using a buffer containing 3 M NaCl, 8 mM NaOH, and 2 mM sarcosyl and UV-cross-linked on the filter. The probes used to detect the presence of the AG-motif and random-sequence transcripts were 5′-TCCCTTCTCCCTTCTCCCCTCC-3′ and 5′-TCTTCTCTTCTTCTCTTCTTCTTC, respectively, labeled with γ [^{32}P] ATP and polynucleotide kinase. For the AG transcript quantification, total RNA was separated in 8% acrylamide/bis-acrylamide (19:1) gel in 7 M urea and TBE and electro-blotted (Multiphor II Novablot Transfer unit, Amersham) as previously described (*28*). The radiolabeled probe that was used, 5′-ATATGTGCTGCCGAAGCGAGCAC, recognized a self-complementary region (GenBank accession no. M14486 bases 1−23) at the 5′ end of both U6 and T-22AG(SCR) transcripts. After hybridization of the sample at 55 °C in a solution containing 1% SDS, 1 M NaCl, 0.2 μg/mL salmon sperm DNA, and 30 ng/mL radiolabeled probe, the filter was exposed to autoradiography and the intensity of the bands was measured with an enhanced laser densitometer (LKB, Bromma, Ultrascan XL).

RNA Isolation and Reverse Transcription−Polymerase Chain Reaction. (A) RNA purification. Cellular mRNA was extracted from the stable transfectants by GenoPrep Direct mRNA kit (GenoVision, Vienna Austria). This method is based on the isolation of mRNA with magnetic beads functionalized with oligo dT. (B) cDNA synthesis. A total of 2.5 μL of mRNA solution in a final volume of 25 μL of diethyl pyrocarbonate (DEPC) water was heated at 70 °C and placed on ice. The solution was added to 25 μL containing (final concentrations) 1× buffer; 0.01 M DTT (Life Technologies, Milan, Italy); 0.8 μM primer dT_{16} (MWG Biotech, Florence, Italy), 0.2 mM dNTPs solution containing

[1] Abbreviations: *pur/pyr*, polypurine/polypyrimidine; Panc-1 cells, human pancreatic adenocarcinoma cells; CD, circular dichroism; PAGE, polyacrylamide gel electrophoresis; GAPDH, glyceraldehyde-3-phosphate dehydrogenase; PCR, polymerase chain reaction; RT, reverse transcriptase.

equimolar amounts of dATP, dCTP, dGTP, and dTTP (Amersham Pharmacia Biotech, Milan, Italy); 0.14 U/μL RNAse inhibitor (Sigma, Milan, Italy); 4 U/μL of M-MLV reverse transcriptase (Life Technologies, Milan, Italy). The reactions (50 μL per tube) were incubated for 1 h at 37 °C and stopped with heating at 95 °C for 5 min. As a negative control, the reverse transcription reaction was performed with 2.5 μL of DEPC water or with RNA but without the enzyme. The cDNA was stored at −20 °C. (C) Polymerase chain reaction (PCR). A volume of 2 μL of cDNA, heated at 95 °C for 5 min, was mixed with the following reagents (final concentrations): 1× Taq buffer with $MgCl_2$ (Eppendorf, Milan, Italy); 0.5 mM $MgCl_2$; 1 μM of each primer; 0.1 mM dNTPs with equimolar amounts of dTTP, dCTP, dATP, dGTP (Amersham Pharmacia Biotech); 0.025 U/μL Taq DNA polymerase (Eppendorf). Amplification was carried out on an automated DNA thermal cycler (Techne, U.K.) as follows: 25 cycles of denaturation (94 °C for 30 s), annealing (55 °C for 30 s) and extension (72 °C for 30 s). Ki-*ras* amplification was carried out with primers Ksx and Kdx (373 bp), while GAPDH amplification was carried out with primers Gsx and Gdx (fragment of 337 bp). Primers were obtained from MWG-Biotech (Florence, Italy): Ksx (5′-GACTGAATATA-AACTTGTGG-3′) 98−117 of exon 1 (GenBank accession no. L00045); Kdx (5′-TGTTTTGT-GTCTACTGTTCT-3′) 375−394 of exon 3 (GenBank accession number L00047); Gsx (5′-AGTATGACAACAGC-CTCAAG-3′) 476−495 (GenBank accession number M33197); Gdx (5′-TTTTCTAGACGGCAGGTCAG-3′) 793−812 (GenBank accession number M33197). The competitor was constructed by PCR in two steps: (i) a 226-bp fragment form pSV2Cat was amplified; (ii) a 266-bp DNA fragment was amplified using primers containing GAPDH and Ki-*ras* sequences. This step provided a 306-bp DNA containing at the termini both GAPDH and Ki-*ras* sequences to be used for amplification. The amplification of this DNA can give rise to either a 266- or a 306-bp fragment depending on the type of primers used. The mRNA quantification was performed as follows. Each RNA sample extracted from the three types of cells was converted into cDNA. To a fixed amount of cDNA were added increasing amounts of competitor. The mixtures were then subjected to PCR to amplify in each sample GAPDH and Ki-*ras* from cDNA and from the competitor. The relative amount of Ki-*ras* mRNA present in the samples was determined by measuring the amounts of cDNA necessary to obtain the equivalence in the intensity of Ki-*ras* and GAPDH bands. The (T/C) × 100 is reported in a histogram. T is Ki-*ras*/GAPDH in either AG or RN tranfectants, while C is the same ratio obtained from untransfected Panc-1 cells.

Growth Curves and Colony Formation Assay. Growth curves were obtained by seeding into 15-mm diameter wells about 5×10^3 cells. Every 2 days, three wells for each clone were trypsinized, and the cells were treated with one volume of Tripan Blue 0.01% in PBS and counted. The results from three independent experiments have been reported in a unique plot showing in ordinate the number of cells and in abscissa the days of growth. For the colony formation assays, 1×10^3 trypsinized cells were seeded on 100-mm diameter plates and grown under normal culture conditions. After 2 weeks, cells were stained with 5% methylene blue in 50% ethanol for 10 min. Colonies constituted by more than 50 cells were counted. Every sample was plated in triplicate and the data reported in an histogram are the average of three independent experiments.

Western Blots. Western blots were performed according to standard procedures. Western blot analyses were performed on total protein lysate in a 2× Laemmli sample buffer (3.3% SDS, 22% glycerol, 1.1 M Tris/HCl, pH 6, 0.001% bromphenol blue, 10% β-mercaptoethanol). Samples were heated at 95 °C for 10 min and about 40 μg were loaded. The relative concentration of the protein lysates was estimated electrophoretically. After separation on 12% SDS−PAGE, equal amounts of lysates were blotted on a nitrocellulose membrane (Sartorius, Germany) by a Multiphor II Novablot Transfer unit (Amersham Pharmacia Biotech, Milan, Italy). Cellular levels of $p21^{RAS}$ and β-actin were measured using commercial available monoclonal antibodies. For $p21^{RAS}$, we used as primary antibody a mouse monoclonal antibody specific for Ki-*ras* p21, used at 3.3 μg/mL (Clone 234−4.2, Oncogene, MA) and as secondary antibody goat anti-mouse IgG (H+L) peroxidase labeled (Euro Clone, U.K.) used at 0.1 μg/mL). For β-actin, we used a commercial actin (Ab-1) kit (Oncogene, MA) (primary antibody used after a dilution of 1:80 000; 100 μg/mL of secondary antibody used at 0.05 μg/mL). Chemiluminescence was detected immediately as described by the manufacturer (Super Signal West Pico, Pierce, Milan, Italy). Films were exposed for about 15 min for Ki-*ras* p21 and 1 min for β-actin.

Electrophoresis Mobility Shift Assays. To detect triplex formation, electrophoresis mobility shift experiments were performed using as a target a 32mer Ki-*ras pur/pyr* duplex and as third strand oligoribonucleotides 22AG and 22SCR. In one set of mixtures, the oligoribonucleotides were radiolabeled with [γ-^{32}P] ATP (Amersham Pharmacia Biotech) and polynucleotide kinase (New England Biolabs, MA) and mixed with increasing amounts of cold 32mer duplex in 50 mM Tris-HCl, pH 8, 5 mM $MgCl_2$, 2.5 mM spermidine, 10% sucrose, 1 U/μL RNase inhibitor (Eppendorf) at 37 °C for 2 h. In another set of mixtures, the Ki-*ras* duplex was radiolabeled and incubated with increasing amounts of cold 22AG or 22SCR. After incubation, the mixtures were run in a native TBE 20% polyacrylamide gel (acrylamide/bisacrylamide = 19/1), thermostated at 25 °C. The gels were dried under reduced pressure at 80 °C and exposed overnight to autoradiography. Protein−nucleic acid binding was analyzed by EMSA in which 5 nM radiolabeled Ki-*ras* duplex or oligoribonucleotide were incubated in 20 μL volume with 1 μg of Panc-1 extract in 20 mM Tris-HCl (pH 8), KCl 100 mM, 1.5 $MgCl_2$, 1 mM DTT, 8% glycerol, for 3 h at room temperature, in the presence or absence of competitor nucleic acid. After incubation, the mixtures were run in a native 5% acrylamide gel in TBE at 12 V/cm, 25 °C. Finally, the gel was dried and autoradiographed. Panc-1 extract of nuclear proteins were obtained as previously described (*29*).

UV Cross-Linking Experiments. Mixtures incubated as described above were placed on ice and irradiated at 5 cm from source using a Vilber-Lourmat BLX 254 cross-linker (or a TFP-M/WL 312 nm UV source). Following irradiation of the sample, the mixtures were run on a 8% polyacrylamide−SDS gel using a standard Tris glycine buffer and visualized by autoradiography.

Immunofluorescence Assay. The cells were fixed with 3% paraformaldehyde in PBS for 1 h at room temperature. Fixed cells were washed with PBS and 0.1 M glycine, pH 7.4, and then permeabilized with 0.1 Triton X-100 in PBS for 5 min. The coverlips were treated with 20 ng/μL of anti-cytochrome c (Promega, Milan, Italy) in PBS for 2 h at 37 °C. Cells were washed with PBS twice, followed by incubation with 62 ng/μL in PBS of FITC-conjugated anti-mouse polyvalent antibody (Sigma) for 30 min at 37 °C. Nuclei were evidenced by Hoechst staining. Cells were examined by LEICA TCS confocal laser microscope equipped with a 488 nm argon laser.

Circular Dichroism (CD) Spectroscopy. CD spectra were recorded at various temperatures using a JASCO J-600 spectropolarimeter. Solutions of oligoribonucleotides (2 μM) were prepared in 50 mM Tris-Cl pH 7.4, 80 mM KCl, 1 mM $MgCl_2$. Spectra were recorded in 0.5-cm quartz cuvette.

RESULTS

Construction of Stable Transfectants Expressing Constitutively AG-Motif Oligoribonucleotides. We used a mammalian expression vector to repress the transcription of the human Ki-*ras* gene in carcinoma pancreatic Panc-1 cells. A 22mer CT-motif sequence was cloned into vector mU6, containing regulatory elements of the human U6 small nuclear RNA gene (*28*). This construct, called pU6−CT, was designed to generate a short transcript (T-22AG) constituted by a central 22mer G-rich element, a 6-bp stem hairpin at the 5′ end, and five uridines at the 3′ end (Figure 1A). The G-rich element, called 22AG, may form alternative secondary/tertiary structures. Indeed, it can form a triplex with a critical *pur*/*pyr* sequence located in the human Ki-*ras* promoter between −148 and −126 from the transcription initiation site (*30*), or, in virtue of its high G-content, it can adopt a tetraplex structure. In addition to pU6−CT, we constructed another expression vector, called pU6−RN, which was used to generate a control transfectant cell line. Vector pU6−RN was designed to drive the synthesis of an AG-motif transcript with a lower G-content (T-22SCR), unable to recognize, via triple-helix formation, the Ki-*ras pur*/*pyr* motif. In this study, we addressed the question whether vector pU6−CT was able to mediate a stable suppression of Ki-*ras* expression in human pancreatic adenocarcinoma Panc-1 cells. To this purpose, Panc-1 cells were cotransfected with vector pCDNA3, bearing the genetycin resistance, and vector pU6−CT (or pU6−RN). Transfected cells were selected with genetycin and the resistant clones were cultivated. After few weeks of growth, we showed by Northern blot analysis that the stable transfectants produced constitutively the expected primary transcripts (Figure 1B). To estimate the number of copies per cell of 22AG-transcript, we compared by Northern blot the amount of T-22AG with the amount of native U6 RNA, using a DNA probe recognizing the self-complementary sequence present in both transcripts (*28*) (Figure 1C). We found that T-22AG was roughly 4% of native U6 RNA. As the number of copies per cell of native U6 RNA is known to be roughly 0.5×10^6 (*31*), the copies per cell of T-22AG should be roughly 2×10^4. If we assume that T-22AG is located in the nucleus and that the nucleus has a diameter of 5 μm, the nuclear concentration of T-22AG is expected to be on the order of 10^{-6}−10^{-7} M.

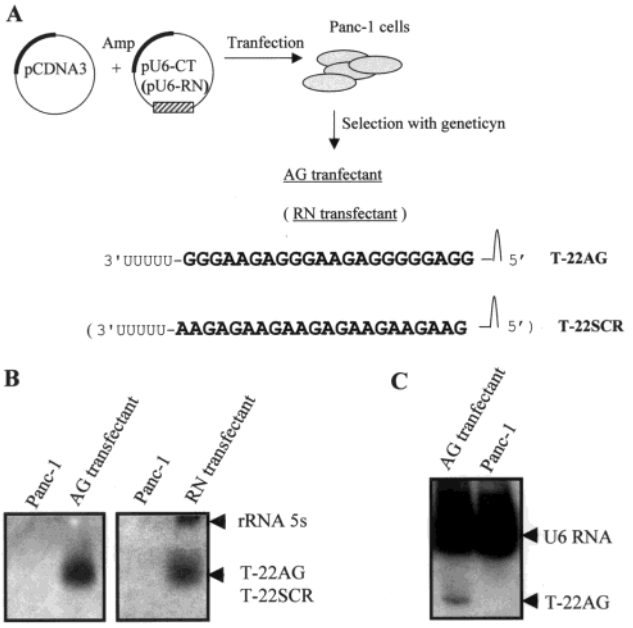

FIGURE 1: (A) Expression vector pU6−CT was obtained from mU6 by insertion of a DNA fragment encoding for a short transcript harboring a 22mer G-rich element (T-22AG). This transcript is potentially capable to self-associate into a tetraplex structure or to form a triple helical complex with a *pur*/*pyr* site located in the promoter of the Ki-*ras* gene. Panc-1 cells have been cotransfected with vector pU6−CT and vector pCDNA3 bearing the genetycin resistance. After selection, resistant clones expressing the expected transcripts were cultivated. Following the same procedure, a control plasmid, pU6−RN, encoding for transcript T-22SCR was obtained. T-22SCR contained a 22-mer AG element that was unable to form a triplex with the Ki-*ras pur*/*pyr* motif; (B) Northern blot demonstrating that the stable transfectants generated the expected transcripts. T-22AG and T-22SCR were detected with radiolabeled probes (5′-TCCCTTCTCCCTTCTCCCCCTCC and 5′-TCTTCTCT-TCTTCTCTTCTTCTTC, respectively) complementary to the central AG-motif stretch; (C) The amount of transcript T-22AG was compared with that of native U6 RNA using a radiolabeled probe recognizing the self-complementary region at the 5′end present in both transcripts (5′-ATATGTGCTGCCGAAGCGAGCAC). Laser scan densitometry analysis showed that T-22AG was about 4% of native U6 RNA.

The Ki-ras Expression in the AG Transfectant is Down-Regulated. The level of Ki-*ras* mRNA in AG transfectant, RN transfectant, and nontransfected Panc-1 cells was determined by a competitive RT-PCR assay. Total RNA extracted from the stable transfectants and from Panc-1 cells were transformed into cDNA, from which two distinct DNA fragments were amplified: a 373-bp fragment from Ki-*ras* and a 334-bp fragment from GAPDH. In addition, we constructed a competitor DNA sharing the same primer recognition sites of cDNA, which gave a 266-bp fragment from the GAPDH primers and a 306-bp fragment from the Ki-*ras* primers. A fixed amount of competitor was added to cDNA, and the mixtures were amplified by PCR. Figure 2 shows that the level of Ki-*ras* mRNA in the AG transfectant was $52 \pm 8\%$ of the control (RN transfectant and nontransfected Panc-1 cells). The reduction of mRNA level is gene-specific as the housekeeping GAPDH gene is equally expressed in all the three different types of cells. Next, we tested by Western blot analysis whether the level of the protein encoded by Ki-*ras* gene, $p21^{RAS}$, was lower in the stable AG transfectant than in the control cells. In Figure 3A we report a typical experiment showing that in the AG trans-

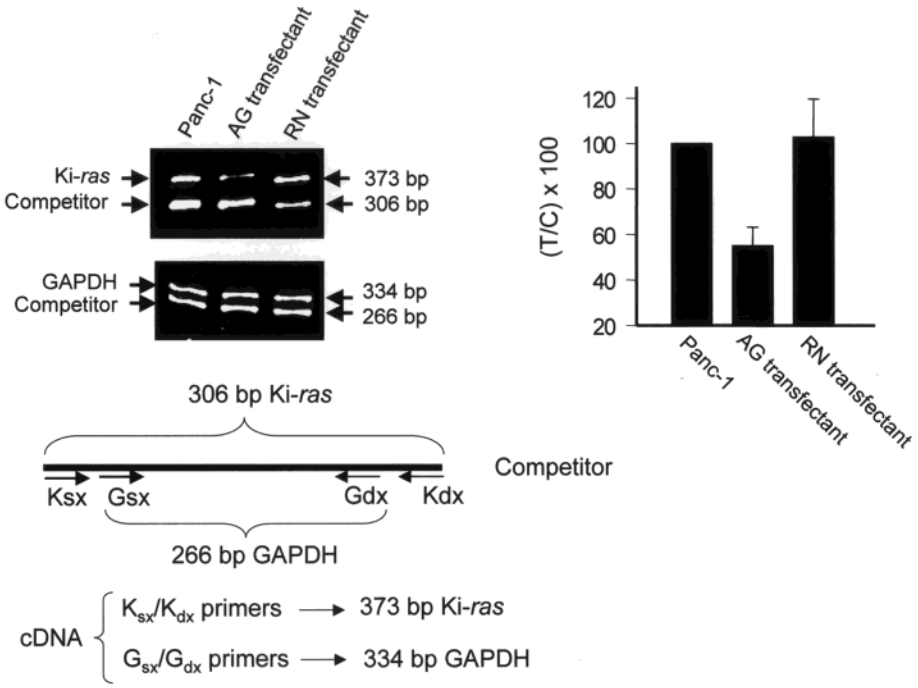

FIGURE 2: Levels of Ki-*ras* mRNA in wild-type Panc-1 cells and in the AG and RN stable transfectants, determined by competitive RT-PCR. Total RNA from wild type and stable transfectants was extracted and subjected to RT. To the resulting cDNA was added a fixed amount of competitor sharing the same Ksx/Kdx and Gsx/Gdx primers of cDNA. Primers Ksx/Kdx were used to amplify a 373-bp fragment from Ki-*ras* cDNA and a 306-bp fragment from the competitor. Primers Gsx/Gdx were used to amplify a 334-bp fragment from GAPDH cDNA and a 266-bp fragment from the competitor DNA. The PCR products have been separated by 8% polyacrylamide gel electrophoresis and the bands stained with ethydium bromide. The histogram shows the level of Ki-*ras* mRNA relative to the level of GAPDH mRNA determined as $(T/C) \times 100$, where T = Ki-*ras*/GAPDH in AG or RN transfectant and C = Ki-*ras*/GAPDH in Panc-1.

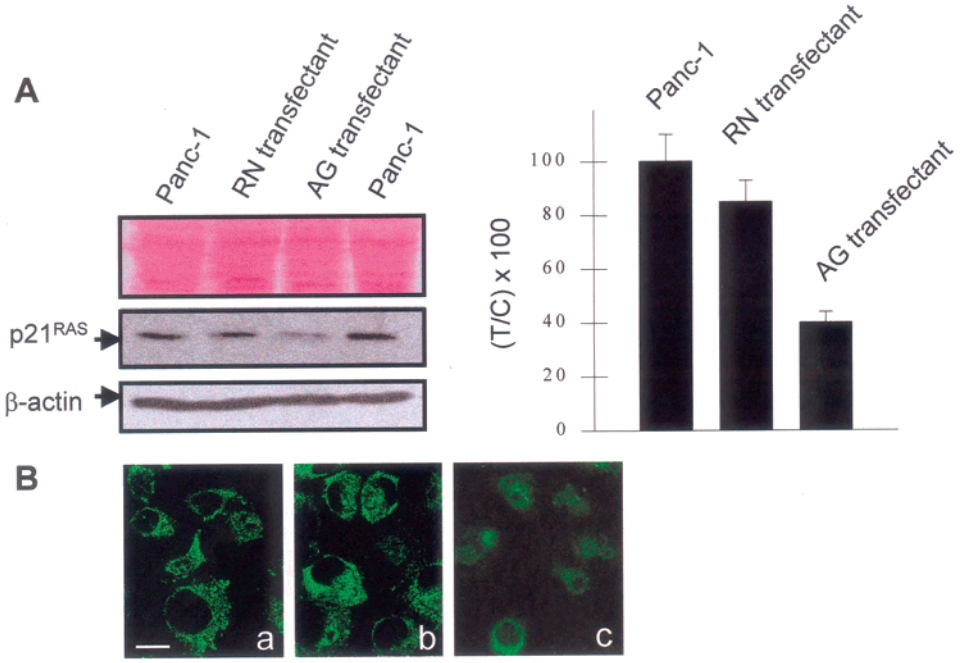

FIGURE 3: Expression of protein $p21^{RAS}$ in Panc-1 and AG and RN transfectants. (A) Western blot of protein lysates isolated from the cell lines. The level of β-actin in each sample was measured as a control. Ponceau S staining of the blotted lysates shows the equivalence of loading. The relative level of $p21^{RAS}$ in the stable transfectants and Panc-1 cells is shown in the histogram. The ordinate reports the T/C ratio, where T is the ($p21^{RAS}/\beta$-actin) ratio in the AG or RN transfectant, while C is the ($p21^{RAS}/\beta$-actin) ratio in Panc-1 cells. (B) Immunofluorescence of cells treated with anti Ki-*ras* and anti mouse fluorescein-conjugated antibodies. Panels a, b, and c show Panc-1, RN-, and AG-transfectant, respectively. Bar, 5 μm.

fectant $p21^{RAS}$ is reduced to 40 ± 4% of the control. This finding is in keeping with the immunofluorescence detection of $p21^{RAS}$, by using an anti-Ki-*ras* antibody (Figure 3B). It can be noted that the level of $p21^{RAS}$ in Panc-1 cells appeared comparable to that in the RN transfectant, but significantly higher than that in the AG transfectant. Taken together, these experiments indicate that the T-22AG promotes a specific inhibition of Ki-*ras* gene expression, as the levels of both mRNA and $p21^{RAS}$ are about half of those normally detected in control RN transfectant and Panc-1 cells.

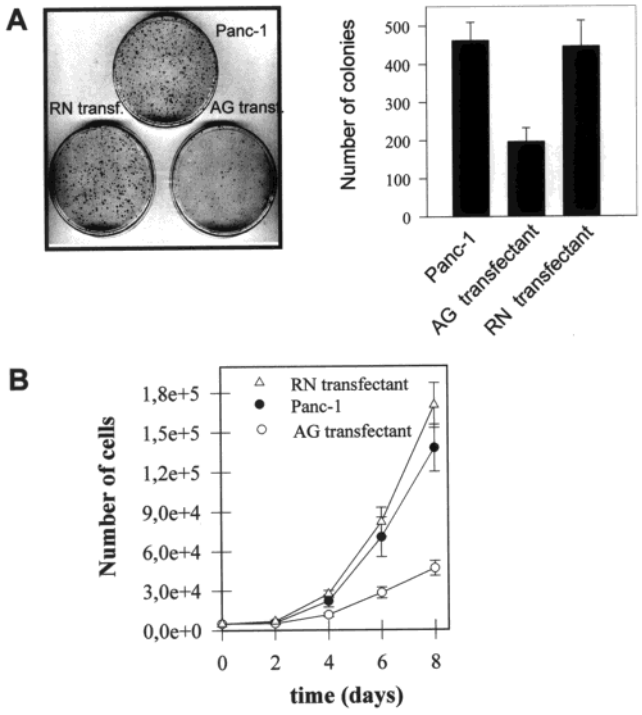

FIGURE 4: (A) Colony-forming assay. Colonies constituted by at least 50 cells were counted after methylene blue staining. The average values of three independent experiments are reported in the histogram; (B) growth curves relative to Panc-1 and AG and RN transfectants. The cells were trypsinized and counted. The average values of three independent experiments are reported in the plot.

Cell Growth and Colony Formation Are Inhibited in the AG Transfectant. Since Ki-*ras* induces cell proliferation, a reduced level of Ki-*ras* expression should cause inhibition of cell growth and colony formation (*5*). Figure 4A shows that T-22AG strongly inhibits the capacity of colony formation by the AG transfectant. The data show that the control cells form colonies that are visible with methylene blue and uniformly distributed in the plate, while the AG transfectant showed a dramatically lower number of colonies. Counting the colonies formed by at least 50 cells, we found that T-22AG promoted a colony formation inhibition of about 60%. The effect of T-22AG on the proliferation of the AG transfectant was evaluated by reporting in a plot the number of cells as a function of time (Figure 4B). Over a period of eight days, the AG transfectant grew more slowly than the control cells: a finding that is in keeping with the colony-forming assay. After eight days, the growth of the AG transfectant was reduced to 34 ± 5% compared with nontransfected Panc-1 cells, or reduced to 27% compared with the RN transfectant. A similar result was observed performing tetrazolium MTT assays (not shown).

Endogenously Generated Transcript Induces Phenotypic Changes of Panc-1 Cells and Apoptosis. The downregulation of Ki-*ras* in the AG transfectant resulted in significant changes in the cell phenotype. While both Panc-1 cells and RN transfectant showed the characteristic cell shape, in the AG transfectant a significant proportion of cells presented a round shape, indicating cell death or, at least, stressed cells (Figure 5A). We found by trypan blue staining that the percentage of nonviable cells normally present in the AG transfectant was roughly 4-times higher (16 ± 2) that that

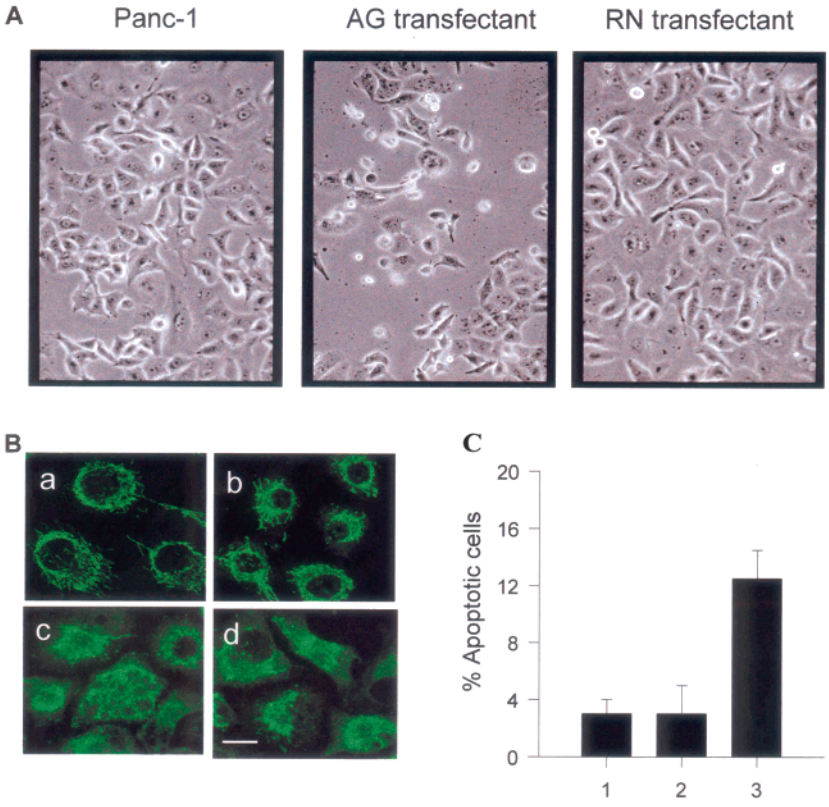

FIGURE 5: (A) Optical microscopy images of Panc-1, AG-, and RN-transfectants. Magnification × 80; (B) immunofluorescence assay performed with anti cytochrome *c* antibody, showing the release of cytochrome *c* from mitochondria: a phenomenon indicative of apoptosis. RN transfectant (a), Panc-1 (b), AG transfectant (c,d); bar, 5 μm; (C) The result of a quantitative analysis showing the percent of apoptotic cells are reported in the histogram. (1) Panc-1 cells; (2) RN transfectant; (3) AG transfectant.

observed in both RN transfectant and Panc-1 cells (2.5 ± 0.5 and 4 ± 0.25%, respectively). Moreover, we examined whether the lower proliferation of the AG transfectant was linked to apoptosis (Figure 5B). It is known that apoptosis is accompanied by release in the cytoplasm of mitochondrial cytochrome *c* (*32*, *33*). Therefore, we analyzed by confocal microscopy the localization of cytochrome *c*, treating the cells with anti-cytochrome *c* and anti-mouse fluorescein-conjugated antibodies. It can be seen in Figure 5B, left, that both Panc-1 cells and RN transfectant showed a filamentous, perinuclear distribution of cytochrome *c*, typical for a mitochondrial localization of cytochrome *c* (panels a and b). In contrast, the AG transfectant showed a release of mitochondrial cytochrome *c* into the cytoplasm, indicative of apoptosis (panels c and d). Moreover, in apoptotic cells the shape of the nuclei stained with Hoechst appeared irregular, with a condensed chromatin. A quantitative analysis of the nuclear shape (apoptosis) in a sample of 500 cells is reported in the histogram (Figure 5C).

Oligonucleotide 22AG Forms a Weak Triplex with the Ki-ras pur/pyr Motif. We assumed that the bioactivity of T-22AG was due to its 22mer G-rich element, as this transcript shares with the nonbioactive T-22SCR both 5′- and 3′-end regions. So, the binding properties of T-22AG were analyzed by using a synthetic RNA fragment representing its G-rich element (22AG). In a first set of experiments, increasing amounts of 22AG were added to a radiolabeled 32mer Ki-*ras pur*/*pyr* duplex, the mixtures were incubated for 3 h at 37 °C and then run in a gel. Following this protocol the binding was not detected (Figure 6, top). We then radiolabeled 22AG and incubated it with increasing amounts of Ki-*ras pur*/*pyr* duplex for 3 h at 37 °C (Figure 6, bottom). In this case, some triplex formation was observed at high DNA/22AG ratios, indicating that 22AG has a low affinity for the Ki-*ras* target. This behavior is likely because 22AG, being a G-rich oligonucleotide, self-associates in solution into an intermolecular tetraplex (vide infra). We also tried to determine whether triplex formation was favored in the presence of nuclear protein extract from Panc-1 cells, as it is known that specific human proteins recognize this particular DNA structure (*34*−*36*). These experiments did not show any triplex stabilization in the presence of increasing amounts of protein extracts. The data suggest that the strong and specific inhibition of Panc-1 growth caused by T-22AG can hardly be attributed to a triplex-based mechanism at the Ki-*ras pyr*/*pyr* motif, considering that the nuclear concentration of T-22AG is expected to be in the order of 10^{-6}/10^{-7} M. So, we addressed the question of how T-22AG could produce such a strong antiproliferative effect in Panc-1 cells. Recent studies have shown that *pur*/*pyr* sequences are associated with tetraplex DNA (*19*, *20*, *37*) and that this unusual DNA conformation can bind to specific cellular proteins (*38*, *39*). Since 22AG has the same sequence, except for the polarity, of the purine strand of the Ki-*ras pur/pyr* motif we addressed the question of whether the G-rich element of T-22AG is capable of interaction with the nuclear proteins that are known to bind to the Ki-*ras pur*/*pyr* motif (*30*, *40*).

The Ki-ras pur/pyr Motif Binds Panc-1 Nuclear Proteins. The Ki-*ras pur*/*pyr* sequence is the target of nuclear proteins (*30*, *40*). Little is known about these proteins, except that they play a critical role on transcription. Thus, we decided

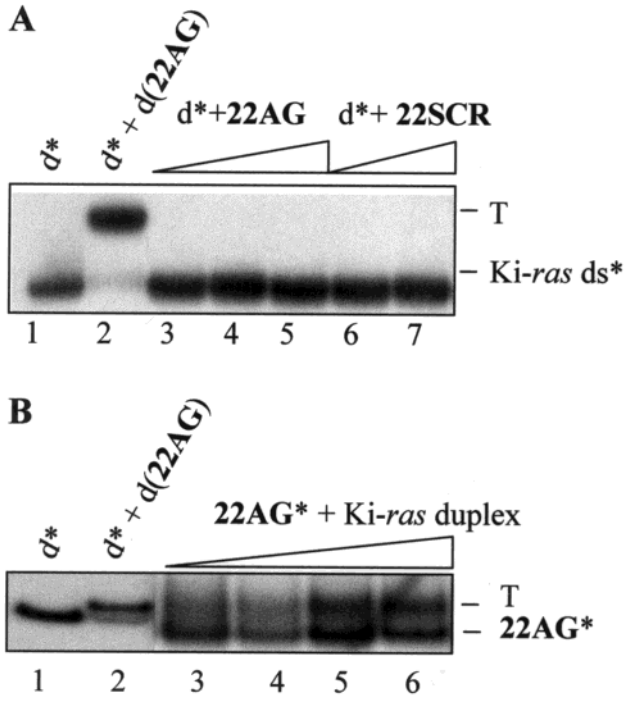

FIGURE 6: EMSA analysis of triplex formation by 22AG and 32mer Ki-*ras pur*/*pyr* duplex (d) at 37 °C, 50 mM Tris-HCl pH 7.4, 5 mM $MgCl_2$, 2.5 mM spermidine, 10% sucrose, 1 U/μL RNase inhibitor. (A) radiolabeled 32mer Ki-*ras pur*/*pyr* duplex was incubated with 1 μM of deoxy 22AG analogue [d(22AG)] (lane 2), 1, 5, 10 μM 22AG (lanes 3−5), 5, 10 μM 22SCR (lanes 6 and 7); (B) radiolabeled 22AG was incubated with 0.1, 1, 5, 10 μM cold Ki-*ras* duplex (lanes 3−6). Lanes 1 shows the mobility of the 32mer Ki-*ras pur*/*pyr* duplex, and lane 2 shows the mobility of the triplex formed by d(22AG).

to perform EMSA with Panc-1 nuclear extract. When increasing amounts (1, 2.5, and 5 μg) of crude nuclear extract were incubated for 30 min with a fixed amount (5 nM) of radiolabeled 32mer Ki-*ras pur*/*pyr* duplex, three retarded bands appeared in the polyacrylamide gel, indicating the formation of three protein−DNA complexes B1, B2, and B3 (Figure 7A). The sequence-specificity of these proteins was examined by competition binding assays. As shown in Figure 7B, a 15- and 35-fold molar excess of unlabeled 32mer Ki-*ras* duplex competed efficiently with the labeled Ki-*ras* duplex (lanes 2 and 3). By contrast, no competition was observed with three nonspecific duplexes, not only at 15- and 35-fold molar excess (lanes 4−8) but also at much higher values (up to 100-fold, not shown). As one of the DNA competitor contained the Sp1 sequence motif (lanes 4 and 5), we concluded that none of the nuclear proteins binding to the human Ki-*ras pur*/*pyr* motif corresponded to the Sp1 transcription factor. Furthermore, we observed that the murine *pur*/*pyr* motif competed with the human motif for binding to the nuclear proteins, as one expects from two DNAs with a high sequence homology (not shown).

The G-rich Element of Transcript T-22AG Competes with the Ki-ras pur/pyr Motif for Protein Binding. We investigated whether 22AG competitively inhibited the interaction between the Ki-*ras pur*/*pyr* motif and the nuclear proteins. The result of the experiment is illustrated in Figure 8A. It can be seen that incubating 1 μg of Panc-1 extract for 30 min with 5 nM labeled 32mer Ki-*ras pur*/*pyr* duplex in the presence of increasing amounts of cold 22AG, in excess over the duplex from 25- to 250-fold, resulted in a concentration-

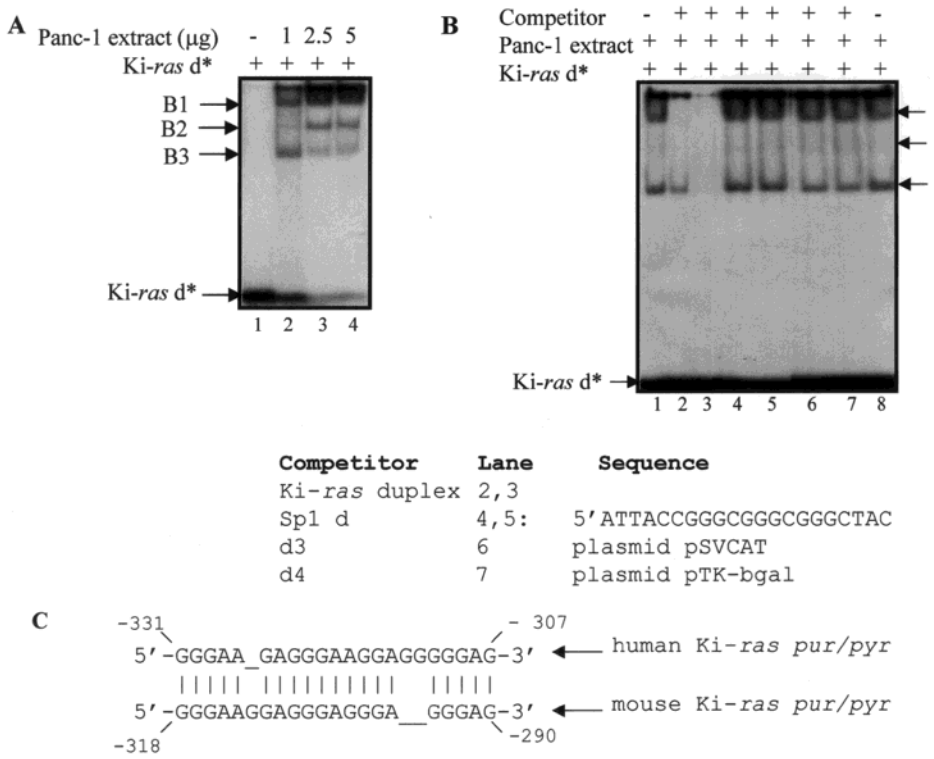

FIGURE 7: (A) EMSA showing the binding of Panc-1 nuclear proteins to the Ki-*ras pur*/*pyr* motif; (B) EMSA showing sequence specificity in the interaction between Panc-1 nuclear proteins and the Ki-*ras pur*/*pyr* sequence; (C) sequence homology between murine and human *pur*/*pyr* motifs.

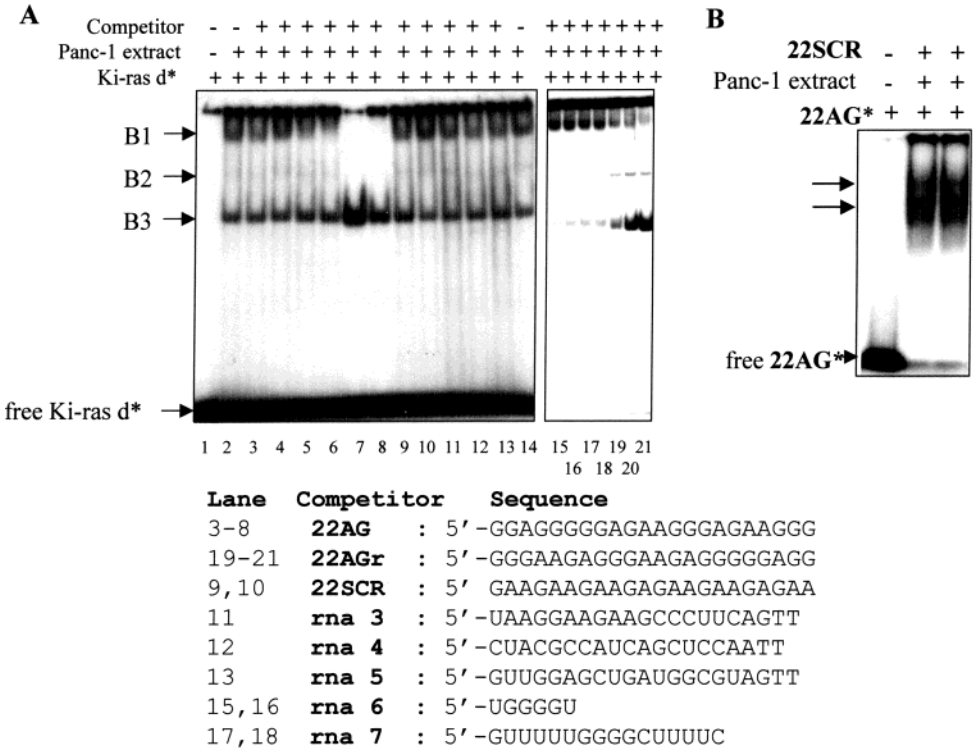

FIGURE 8: EMSA showing that 22AG competitively binds to a nuclear factor recognizing the Ki-*ras pur*/*pyr* motif. Competitor 22AG in lanes 3−8 was 15/35/60/130/200/260-fold in excess over the Ki-*ras* duplex. The sequences of the RNA competitors used in lanes 9−21 are shown. Competitor 22AGr in lanes 19−21 was 50/125/250-fold in excess over the Ki-*ras pur*/*pyr* motif duplex. (B) EMSA showing that 22AG incubated with 1 μg of Panc-1 extract and in the presence of 100-fold excess 22SCR forms two RNA−protein complexes.

dependent inhibition of the interaction between the protein of complex B1 and labeled Ki-*ras pur*/*pyr* duplex. An inhibition of 50% is obtained with 22AG at about 50-fold molar excess (~250 nM), suggesting that 22AG has a high affinity for this DNA-binding nuclear factor. The interaction between 22AG and the protein in complex B1 is sequence specific as no competition was observed with a number of RNA molecules including 22SCR, i.e., the AG-motif element of transcript T-22SCR, RNAs forming G-quartet structures (rna-6 and rna-7) (*41*, *42*) and RNAs with random sequences

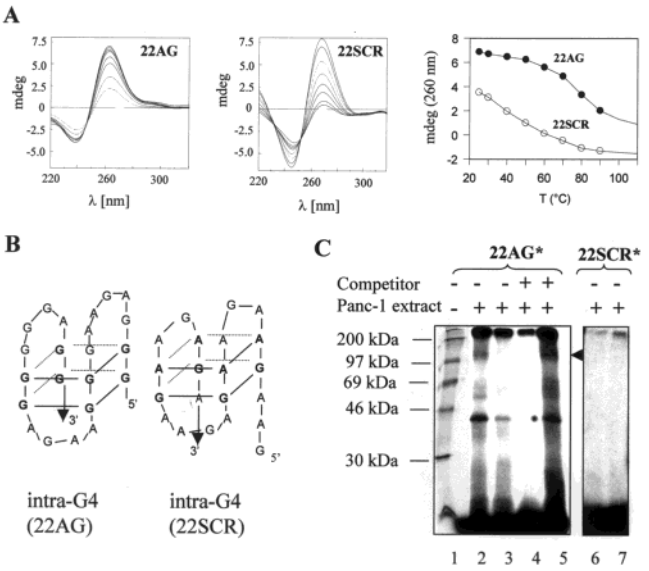

FIGURE 9: (A) Circular dichroism spectra as a function of temperature of 2 μM 22AG and 22SCR. Melting profiles have been obtained plotting the ellipticity at 260 nm as a function of temperature; (B) possible intramolecular tetraplexes that can be formed by oligonucleotides 22AG and 22SCR; (C) SDS−PAGE (8%) of 1 μg Panc-1 extract after UV cross-linking in the presence of radiolabeled 22AG (lane 2); heated radiolabeled 22AG (lane 3); radiolabeled 22AG in the presence of excess Ki-*ras* duplex (lane 4); radiolabeled 22AG in the presence of excess 22SCR (lane 5); radiolabeled 22SCR (lane 6); radiolabeled 22SCR mixed with 2 μg of extract (lane 7). Lane 1 shows the migration of the protein markers.

(rna-3, rna-4, rna-5). Moreover, the experiment showed that (i) there is no competition between 22AG and the Ki-*ras pur*/*pyr* motif for binding to the protein in the B3 complex; (ii) the interaction between the protein in complex B2 and the Ki-*ras pur*/*pyr* motif is weak under the conditions used, so that we did not take it into consideration; (iii) 22AGr, the reverse sequence of 22AG, also competes for protein binding as does 22AG. Next, we incubated radiolabeled 22AG with Panc-1 extract for 30 min to detect directly the binding between 22AG and the nuclear proteins (Figure 8B). It can be seen that in the presence of a large amount of cold 22SCR, to suppress sequence-independent interactions, 22AG appeared to bind to two proteins of the Panc-1 extract.

The G-rich Element of T-22AG Adopts a Tetraplex Conformation. We addressed the question whether the interaction between the nuclear factor and T-22AG was mediated by the possible structure that can be adopted by the G-rich element 22AG. So the capacity of 22AG to form unusual tertiary structures in solution was investigated by circular dichroism (CD). CD spectroscopy is sensitive to base stacking in DNA and RNA (*43*). Figure 9A shows the CD spectra of 22AG and 22SCR (2 μM) in 30 mM Tris-HCl pH 7.4, 80 mM KCl, 5 mM $MgCl_2$. The spectra are similar in the 220−290 region, with a strong and positive peak at ∼264 nm and a negative peak at ∼245 nm, and they are different in the 290−310 nm region, where only 22AG shows a small shoulder at 295 nm. A CD spectrum characterized by a large 264-nm peak has been attributed to parallel tetraplex structures (*44*, *45*). However, there are oligonucleotides forming folded antiparallel tetraplexes, such as d(GGGTGGGTGGGTGGGT) (*46*) and d(TTTGGTGGTG-GTGGTTGTGGTGGTGGTGG) (*47*), that also exhibit this type of spectrum. Thus, the CD spectra show that 22AG and 22SCR adopt a G-quartet structure, but do not provide indications about the molecularity. The intensity of the 264 nm peak is strongly reduced by increasing the temperature, suggesting the presence of extensive base stacking in both 22AG and 22SCR. However, plotting the ellipticity at 260 nm as a function of temperature we obtained two melting curves that should reflect a single-strand ⇔ tetraplex equilibrium (Figure 9A). It is noteworthy that 22AG exhibits a cooperative transition with a T_m between 75 and 80 °C, while 22SCR shows a low-cooperative melting profile with T_m around 40 °C. In a native polyacrylamide gel, both oligonucleotides migrated with a fast-moving band and with a smeared slow-moving band (not shown). Taken together, these data indicate that both oligonucleotides adopt in solution either a parallel or a folded tetraplex conformation which is stabilized by G- (*44*) and A-tetrads (*48*) (Figure 9B). We also found as expected that the CD spectrum of 22AGr, the reverse sequence of 22AG, is practically identical to that of 22AG (not shown).

Next, we investigated whether the protein in the complex B1 was recognized by the primary or tertiary structure of 22AG. To this aim, we performed PAGE/UV cross-linking experiments as illustrated in Figure 9C. We incubated for 30 min 1 μg of Panc-1 extract with 5 nM radiolabeled 22AG which was left in its conformation (lane 2) or denatured at 90 °C (lane 3). We tested the effect on the binding of 22AG to the nuclear proteins of 100-fold excess competitors such as Ki-*ras pyr*/*pyr* duplex (lane 4) or 22SCR (lane 5). As a control, we radiolabeled and mixed with the extract 22SCR (lanes 6 and 7). After 30 min incubation, the mixtures were irradiated at 256 nm for 5 min. The oligonucleotide−protein complexes were then separated by SDS−12% PAGE. It can be seen that (i) the interaction between 22AG and the nuclear proteins gives rise to three major complexes with apparent molecular masses of 120, 60, and 40 kDa; (ii) the thermal treatment abrogates the 120 and 60 kDa complexes but not that of 40 kDa, indicating that when 22AG is unstructured, it largely loses its binding capacity; (iii) the Ki-*ras pur*/*pyr* duplex competes with 22AG to bind to the proteins (lane 4), while 22SCR does not (lane 5); (iv) 22SCR does not bind to any of the nuclear proteins. In addition, we performed UV cross-linking experiments in which the Ki-*ras pur*/*pyr* sequence was radiolabeled and a number of DNA and RNA sequences were used as competitors. We found that the Ki-*ras* duplex formed a DNA−protein complex of 112 kDa, which was competed by 22AG but not by 22SCR (not shown). Collectively, these data indicate that the protein in complex B1 (whose apparent molecular weight was estimated to be about 90 kDa) is able to bind not only to the Ki-*ras pur*/*pyr* motif but also to the tetraplex-forming 22AG sequence.

DISCUSSION

In this study, we have demonstrated that an endogenously generated transcript containing a G-rich element specifically downregulated the expression of the Ki-*ras* oncogene and strongly inhibited the capacity of growth and colony formation of pancreatic carcinoma Panc-1 cells. As protein $p21^{RAS}$ conveys mitogenic signals from the cell surface to the nucleus, its depletion causes dramatic effects on cell biology (*49*, *50*). Moreover, as observed in primary keratinocytes

(*51*), a reduced level of Ki-*ras* expression results in changes of cell morphology. The G-rich element of transcript T-22AG was designed with a sequence equal but antiparallel to the purine strand of the *pur*/*pyr* motif located in the Ki-*ras* promoter, which is about 13 helical turns from transcription initiation. Our data indicate that the strong antiproliferative effect promoted by T-22AG did not correlate with triplex formation at the critical Ki-*ras pur*/*pyr* motif, but to its capacity to interact specifically with a nuclear protein, normally binding to the Ki-*ras pur*/*pyr* motif. This is supported by the fact that the AG element of T-22AG specifically binds to a nuclear protein and forms with the *pur*/*pyr* target a triplex, which is weak even under favorable ionic conditions (absence of K^+ ions). However, although our data strongly support this picture, we cannot totally exclude that in vivo polyamine levels facilitate triplex formation and make this structure bioactive. CD experiments showed that the AG-elements of transcripts T-22AG and T-22SCR assume a tetraplex structure. Four-stranded structures are normally stabilized by G-tetrads (*45*) but also A-tetrads have been described (*48*). The higher stability of the tetraplex formed by 22AG is probably because it contains more G-tetrads than the tetraplex formed by 22SCR. It is possible that the low capacity of 22AG to form a triplex with the Ki-*ras pur*/*pyr* motif is due to its inherent tendency to assume a tetraplex conformation. This is in keeping with the fact that a small amount of triplex was observed when 22AG was radiolabeled and mixed at a low concentration with the Ki-*ras pur*/*pyr* duplex, i.e., under experimental conditions that did not favor self-association. While triplex formation by pyrimidine oligoribonucleotides has been well documented (*52*−*54*), triplex formation by purine oligoribonucleotides has not been thoroughly investigated and has been reported only for targets in murine Ki-*ras* (*14*) and rat alpha-1 (I) (*55*) genes. Interestingly, we found that 22AG competitively inhibited the binding between a Panc-1 nuclear factor and the Ki-*ras pur*/*pyr* sequence. The human Ki-*ras pur*/*pyr* sequence is located within −400/−250 relative to exon 0/intron 1, was shown to be a nuclease hypersensitive site, and represents an essential regulatory element of the human Ki-*ras* gene (*18*). The human Ki-*ras* promoter shares 82% sequence homology with the murine analogue, which also contains a *pur*/*pyr* motif at a very similar location, i.e., from −290 to −318 relative to exon 0/intron 1 (*56*). The murine *pur*/*pyr* motif has been shown to bind to three HeLa nuclear factors, as observed with the human motif, and to cause a total loss of promoter activity upon deletion (*40*). Due to their high sequence homology, the murine and human Ki-*ras pur*/*pyr* motifs compete with each other for binding to the same nuclear proteins in HeLa (*30*) and Panc-1 (this study) extracts. These data argue that both human and murine *pur*/*pyr* motifs are important protein-binding sites that are essential for transcription. The binding of the nuclear proteins to the human Ki-*ras* motif is highly sequence-specific, as a number of duplexes, including that containing the Sp1 consensus sequence, did not compete for protein binding. Since T-22AG promoted a strong inhibition of cell proliferation and at the same time exhibited, under in vitro conditions, a weak capacity of triplex formation, we addressed the question of whether this unnatural RNA acted as a molecular aptamer for one of the nuclear proteins binding to the Ki-*ras pur*/*pyr* motif. This hypothesis is supported by the fact that (i) recent studies have shown that polypurine G-rich DNA or RNA strands can promote specific interactions with cellular proteins (*57*−*60*); (ii) tetraplex structures are associated to nuclease hypersensitivity *pur*/*pyr* motifs present in the regulatory region of many genes (*19*, *20*). Indeed, we found that 22AG competed with the Ki-*ras pur*/*pyr* duplex for binding to the nuclear protein showing the lower mobility in the EMSA assay. About 50% of inhibition was observed at an oligoribonucleotide concentration as low as 50 nM, indicating that 22AG has a high affinity for this nuclear protein. The oligonucleotide−protein interaction appeared to be sequence-specific as a number of control oligoribonucleotides, including 22SCR which also form a tetraplex, did not compete with the Ki-*ras pur*/*pyr* duplex, even when they were used in 100-fold excess. By contrast, the addition of increasing amounts of cold 22AG to mixtures containing radiolabeled Ki-*ras pur*/*pyr* duplex and Panc-1 extract, resulted in a concentration-dependent inhibition of the interaction between the protein in complex B1 and radiolabeled Ki-*ras* duplex. Cold 22AG did not compete with the Ki-*ras* duplex for binding to the protein giving rise to complex B3. These results argue strongly that the protein in complex B1 is a DNA-binding protein that appears to have a sequence specific-affinity for the G-rich oligonucleotide 22AG. A direct demonstration that 22AG binds specifically to Panc-1 nuclear proteins was obtained by incubating radiolabeled 22AG with Panc-1 extract, in the presence of excess RNA competitor (22SCR). By means of UV cross-linking and SDS−PAGE, we roughly evaluated that the molecular mass of the nuclear factor binding to the Ki-*ras pur*/*pyr* motif and oligonucleotide 22AG is approximately 90 kDa [120 kDa (complex) − 30.8 kDa (tetraplex 22AG)]. Moreover, UV-cross-linking assays performed in the presence of specific DNA and RNA competitors demonstrated that the protein which competitively recognized both the Ki-*ras pur*/pyr motif and 22AG is that of complex B1. Interestingly, we found that the interaction between the nuclear factor and 22AG appeared to be mediated by a tetraplex conformation, as heating 22AG at 95 °C for 2 min entirely abrogated the interaction with the protein. G-rich oligonucleotides forming tetraplex structures have been shown to bind specifically to cellular proteins. For instance, a guanosine-rich 15mer oligonucleotide forming a highly compact tertiary structure including two layers of G tetrads was found to bind and inhibit the human blood-clotting factor thrombin (*61*); 28mer RNA and DNA oligonucleotides harboring G4 domains bound specifically yeast protein G4p2 (39); a G-rich DNA forming mixed guanine and adenosine quartets bound to L-arginine (*62*); a G-quartet forming oligoribonucleotide was found to bind to the N-terminal amino acids 23−52 from Syrian golden hamster prion protein PrP (*57*). These examples suggest that G-quartet represents a recurring structural motif, which is recognized by several proteins. However, the fact that G-rich nucleic acids bind specifically to different proteins, despite that they all form tetraplex structures, suggests that the binding is complex and seems to depend on subtle structural features of the quadruplex and on specific nucleobase-amino acid contacts. This is in keeping with the observations that 22SCR, rna-6 and rna-7 did not bind to the nuclear factor in complex B1 despite they adopt a tetraplex conformation. The finding that oligonucleotide 22AG specifically interacted with a Panc-1

nuclear factor correlates with the structural polymorphism associated to *pur*/*pyr* motifs in DNA. *pur*/*pyr* motifs are important elements located in the 5′ flanking regions of many genes that exhibit nuclease hypersensitivity. It has been shown that the nuclease hypersensitivity elements in c-*myc*, Ki-*ras*, c-*myb*, and PDGF-A (*19*) are capable of engaging in a slow duplex-to-tetraplex equilibrium (*19*, *20*). It is therefore possible that the 90-kDa nuclear factor has an inherent capacity to specifically recognize both duplex and tetraplex conformations of the Ki-*ras pur*/*pyr* motif. Although 22AG has the opposite polarity, its sequence corresponds to purine strand of the Ki-*ras pur*/*pyr* motif and forms a G-quartet structure. So, T-22AG likely behaves as an aptamer for the 90-kDa nuclear factor. In conclusion, the results of this study suggest that, in addition to the molecular strategies so far proposed to inhibit the expression of the Ki-*ras* gene in tumor cells, a strategy based on the use of aptamer molecules capable to specifically interact with the nuclear factors binding to the *pur*/*pyr* motif appears to be very attractive.

ACKNOWLEDGMENT

We are grateful to Dr. Sarah Noonberg (University of San Francisco) for supplying vector mU6.

REFERENCES

1. Gunzburg, W. H., and Salmons, B. (2001) Novel clinical strategies for the treatment of pancreatic carcinoma. *Trends Mol. Med. 7*, 30−37.
2. Bardeesy, N., and DePinho, R. A. (2002) Pancreatic cancer biology and genetics. *Nat. Rev. 2*, 897−909.
3. Alberts, B., Johson, A., Lewis, J., Raff, M., Roberts, K., and Walter, P. (2002) Molecular biology basis of cancer cell behaviour, in *Molecular Biology of the Cell*, 4th ed., pp 1340−1355, Garland Science, New York.
4. McCormick, F. (1989) Ras GTPase activating protein: signal transmitter and signal terminator. *Cell 56*, 5−8.
5. Bos, J. L. (1989) Ras oncogenes in human cancer: a review. *Cancer Res. 49*, 4682−4689.
6. Kamai, T., Araqi, K., Koga, F., Abe, H., Nakanishi, K., Kambara, T., Furuya, N., Tsujii, T., and Yoshida, K. I. (2001) Higher expression of Ki-*ras* is associated with parathyroid hormone-related protein-induced hypercalcaemia in renal cell carcinoma. *BJU Int. 88*, 960−966.
7. Kozma, L., Kiss, I., Hagy, A., Szakall, S., and Ember, I. (1997) Investigation of c-myc and Ki-*ras* amplification in renal clear cell adenocarcinoma. *Cancer Lett. 111*, 127−131.
8. Liu, M. L., Von Lintig, F. C., Liyanage, M., Shibata, M. A., Jorcyk, C. L., Ried, T., Boss, G. R., and Green, J. E. (1998) Amplification of Ki-*ras* and evaluation of MAP kinase activity during mammary tumor progression in C3 (1)/SV40 Tag transgenic mice. *Oncogene 17*, 2401−2411.
9. Chin, L., Tam, A., Pomerantz, J., Wong, M., Holash, J., Bardeesy, N., Shen, Q., O'Hagan, R., Pantginis, J., Zhou, H., Horner, J. W., 2nd, Cordon-Cardo, C., Yancopoulos, G. D., and DePinho, R. A. (1999) Essential role for oncogenic Ras in tumour maintenance. *Nature 400*, 468−472.
10. Downward, J. (2003) Targeting ras signaling pathways in cancer therapy. *Nat. Rev. Cancer 3*, 11−22.
11. Kita, K., Saito, S., Morioka, C. Y., and Watanabe, A. (1999) Growth inhibition of human pancreatic cancer cell lines by antisense oligonucleotides specific to mutated K-*ras* gene. *Int. J. Cancer 80*, 553−558.
12. Aoki, K., Yoshida, T., Matsumoto, N., Ide, H., Sugimura, T., and Terada, M. (1997) Suppression of Ki-ras p21 levels leading to growth inhibition of pancreatic cancer cell lines with Ki-ras mutation but not those without Ki-ras mutation. *Mol. Carcinog. 20*, 251−308.
13. Giannini, C. D., Roth, W. K., Piper, A., and Zeuzem, S. (1999) Enzymatic and antisense effects of a specific anti-ki-ras ribozymes in vitro and in culture cells. *Nucleic Acids Res. 27*, 2737−2744.
14. Cogoi, S., Suraci, C., Del Terra, E., Diviacco, S., van der Marel, G., van Boom, J., Quadrifoglio, F., and Xodo, L. E. (2000) Downregulation of c-Ki-*ras* promoter activity by triplex-forming oligonucleotides endogenously generated in human 293 cells. *Antisense Nucleic Acid Drug Dev. 10*, 283−295.
15. Cogoi, S., Rapozzi, V., Quadrifoglio, F., and Xodo, L. E. (2001) Anti-gene effect in live cells of AG motif triplex-forming oligonucleotides containing an increasing number of phosphorothioate linkages. *Biochemistry 40*, 1135−1143.
16. Cogoi, S., Rapozzi, V., and Xodo, L. E. (2003) Inhibition of gene expression by peptide nucleic acids in cultured cells. *Nucleosides Nucleotides Nucleic Acids 22*, 1615−17.
17. Sebti, S. M., and Hamilton, A. D. (2000) Farnesyltransferase and geranylgeranyl-transferase I inhibitors and cancer therapy: Lessons from mechanmism and bench-to-bedside translational studies. *Oncogene 19*, 6584−6593.
18. Jordano, J., and Perucho, M. (1986) Chromatin structure of the promoter region of the human c-K-ras gene. *Nucleic Acids Res. 14*, 7361−7368.
19. Saddiqui-Jain, A., Grand, C. L., Bears D. J., and Hurley, L. H. (2002) Direct evidence for a G-quadruplex in a promoter region and its targeting with a small molecule to repress c-*myc* transcription. *Proc. Natl. Acad. Sci. U.S.A. 99*, 11593−11598.
20. Simonsson, T., Pecinka, P., and Kubista, M. (1998) DNA tetraplex formation in the control region of c-*myc*. *Nucleic Acids Res. 26*, 1167−1172.
21. Cooney, M., Czernuszewicz, G., Postel, E. H., Flint, S. J., and Hogan, M. E. (1988) Site-specific oligonucleotide binding represses transcription of the human c-*myc* gene in vitro. *Science 241*, 456−459.
22. Vasquez, K. M., and Wilson, J. H. (1998) Triplex-directed modification of genes and gene activity. *Trends Biochem. Sci. 23*, 4−9.
23. Beal, P. A., and Dervan, P. B. (1991) Second structural motif for recognition of DNA by oligonucleotide directed triple helix formation. *Science 251*, 1360−1363.
24. McGuffie, E. M., Pacheco, D., Carbone, G. M. R., and Catapano, C. V. (2000) Antigene and antiproliferative effects of a c-*myc*-targeting phosphorothioate triple helix-forming oligonucleotide in human leukaemia cells. *Cancer Res. 60*, 3790−3799.
25. Duval-Valentin, G., Thuong, N. T., and Hélène, C. (1992) Specific inhibition of transcription by triple helix-forming oligonucleotides. *Proc. Natl. Acad. Sci. U.S.A. 89*, 504−508.
26. Alunni-Fabbroni, M., Pirulli, D., Manzini, G., Xodo, L. E. (1996) (A,G)-oligonucleotides form extraordinary stable triple helices with a critical R.Y sequence of the murine c-Ki-ras promoter and inhibit transcription in transfected NIH 3T3 cells. *Biochemistry 35*, 16361−16369.
27. Lieber, M., Mazzetta, J., Nelson-Rees, W., Kaplan, M., and Todaro, G. (1975) Establishment of a continuous tumor-cell line (panc-1) from a human carcinoma of the exocrine pancreas. *Int. J. Cancer 15*, 741−747.
28. Noonberg, S. B., Scott, G. K., Garovoy, M. R., Benz, C. C., and Hunt, C. A. (1994) In vivo generation of highly abundant sequence-specific oligonucleotides for antisense and triplex gene regulation. *Nucleic Acids Res. 22*, 2830−2836.
29. Dignam, J. D. (1990) Preparation of extracts from higher eukaryotes. *Methods Enzymol. 182*, 194−203.
30. Mayfield, C., Squibb, M., and Miller, D. (1994) Inhibition of nuclear protein binding to the human K-ras promoter by triplex-forming oligonucleotides. *Biochemistry 33*, 3358−3363.
31. Sauterer, R., Feeney, R., and Zieve, G. (1988) Cytoplasmic assembly of snRNP particles from stored proteins and newly transcribed snRNA's in L929 mouse fibroblasts. *Expr. Cell Res. 176*, 344−359,
32. Li, K., Li, Y., Shelton, J. M., Richardson, J. A., Spencer, E., Chen, Z. J., Wang, X., and Williams, R. S. (2000) Cytochrome *c* deficiency causes embryonic lethality and attenuates stress-induced apoptosis. *Cell 101*, 389−399.
33. Paroni, G., Henderson, C., Schneider, C., and Brancolini, C. (2001) Caspase-2-induced apoptosis is dependent on caspase-9, but its processing during UV- or tumor necrosis factor-dependent cell death requires caspase-3. *J. Biol. Chem. 276*, 21907−21915.
34. Kiyama, R., and Camerini-Otero, R. D. (1991) A triplex DNA-binding protein from human cells: purification and characterization. *Proc. Natl. Acad. Sci. U.S.A. 88*, 10450−10454.
35. Guieyesse, A. L., Praseuth, D., and Hélène, C. (1997) Identification of a triplex DNA-binding protein from human cells. *J. Mol. Biol. 267*, 289−298.

36. Musso, M., Nelson, L. D., and Van Dyke, M. W. (1998) Characterization of purine-motif triplex DNA-binding proteins in HeLa extracts. *Biochemistry 37*, 3086−3095.
37. Rangan, A., Fedoroff, O. Y., and Hurley, L. H. (2001) Induction of duplex to G-quartet transition in the c-myc promoter region by a small molecule. *J. Biol. Chem. 276*, 4640−4646.
38. Arthanari, H., and Bolton, P. H. (2001) Functional and dysfunctional roles of quadruplex DNA in cells. *Chem. Biol. 8*, 221−230.
39. Frantz, J. D., and Gilbert, W. (1995) A yeast gene product, G4p2, with a specific affinity for quadruplex nucleic acids. *J. Biol. Chem. 270*, 9413−9419.
40. Hoffman, E. K., Trusko, S. P., Murphy, M., and George, D. L. (1990) An S1 nuclease-sensitive homopurine/homopyrimidine domain in the c-Ki-ras promoter interacts with a nuclear factor. *Proc. Natl. Acad. Sci. U.S.A. 87*, 2705−2709.
41. Oliver, A. W., and Kneale, G. G. (1999) Structural characterization of DNA and RNA sequences recognised by the gene 5 protein of bacteriophage fd. *Biochem. J. 339*, 525−531.
42. Cheong, C., and Moore, P. B. (1992) Solution structure of an unusually stable RNA tetraplex containing G- and U-quartet structures. *Biochemistry 31*, 8406−8414.
43. Gray, D. M., and Tinoco, I., Jr. (1970) A new approach to the study of sequence-dependent properties of polynucleotides. *Biopolymers 9*, 223−244.
44. Giraldo, R., Suzuki, M., Chapman, L., and Rhodes, D. (1994) Promotion of parallel Quadruplexes by yeast telomere binding proteins: a circular dichroism study. *Proc. Natl. Acad. Sci. U.S.A. 91*, 7658−7662.
45. Williamson, J. R. (1994) G-quartet structures in telomeric DNA. *Annu. Rev. Biophys. Biomol. Struct. 23*, 607−611.
46. Jing, N., and Hogan, M. E. (1998) Structure−activity of tetrad-forming oligonucleotides as a potent anti-HIV therapeutic drug. *J. Biol. Chem. 273*, 34992−34999.
47. Dapic, V., Abdomerovic, V., Marrington, R., Peberdy, J., Rodger, A., Trent, J. O., and Bates, P. J. (2003) Biophysical and biological properties of quadruplex oligodeoxyribonucleotides. *Nucleic Acids Res. 31*, 2097−2107.
48. Patel, P. K., Koti, A. S. R., and Hosur, R. V. (1999) NMR studies on truncated sequences of human telomeric DNA: observation of a novel A-tetrad. *Nucleic Acids Res. 27*, 3836−3843.
49. Aoki, K., Yoshida, T., Matsumoto, N., Ide, H., Sugimura, T., and Terada, M. (1997) Suppression of Ki-ras p21 levels leading to growth inhibition of pancreatic cancer cell lines with Ki-ras mutation but not those without Ki-ras. *Mol. Carcinog. 80*, 553−558.
50. Macaluso, M., Russo, G., Cinti, C., Bazan, V., Gebbia, N., and Russo, A. (2002) Ras family genes: an interesting link between cell cycle and cancer. *J. Cell Physiol. 192*, 125−130.
51. Hoa, M,. Davis, S. L., Ames, S. J., and Spanjaard, R. A. (2002) Amplification of wild-type K-ras promotes growth of head and neck squamous cell carcinoma. *Cancer Res. 62*, 715−716.
52. Wang, S., and Kool, E. T. (1995) Origins of the large differences in stability of DNA and RNA helices: C-5 methyl and 2′-hydroxyl effects. *Biochemistry 34*, 4125−4132.
53. Escude, C., Francois, J. C., Sun, J. S., Ott, G., Sprinzl, M., Garestier, T., and Hélène, C. (1993) Stability of triple helices containing RNA and DNA strands: experimental and molecular modeling studies. *Nucleic Acids Res. 21*, 5547−5553.
54. Roberts, R. W., and Crothers, D. M. (1992) Stability and properties of double and triple helices: dramatic effects of RNA or DNA backbone composition. *Science 258*, 1463−1466.
55. Ririe, S. S., and Guntaka, R. V. (1998) An RNA oligonucleotide corresponding to the polypyrimidine region of the rat alpha 1(I) procollagen promoter forms a stable triplex and inhibits transcription. *Biochem. Biophys. Res. Commun. 249*, 218−221.
56. McGrath, J. P., Capon, D. J., Smith, D. H., Chen, E. Y., Seeburg, P. H., and Goeddel, D. V. (1983) Structure and organization of the human Ki-ras proto-oncogene and a related processed pseudogene. *Nature 304*, 501−506.
57. Weiss, S., Proske, D., Neumann, M., Groschup, M. H., Kretzscmar, H. A., Famulok, M., and Winnacker, E. L. (1997) RNA aptamers specifically interact with the prion protein Pr. *J. Virol. 71*, 8790−8797.
58. Suzuki, J., Miyano-Kurosaki, N., Kuwasaki, T., Takeuchi, H., Kawai, G., and Takaku, H. (2002) Inhibition of human immunodeficiency virus type I activity in vitro by a new self-stabilised oligonucleotide with guanosine-thymidine quaqdruplex motifs. *J. Virol. 76*, 3015−3022.
59. Tam, R. C., Lin, C. J. L., Lim, C., Pai, B., and Stoisavljevic, V. (1999) Inhibition of CD28 expression by oligonucleotide decoys to the regulatory element in exon 1 of the CD28 gene. *J. Immunol. 163*, 4292−4299.
60. Marchand, C., Pourquier, P., Laco, G. S., Jing, N., and Pommier, Y. (2002) Interaction of human topoisomerase I with guanosine quartet-forming and guanosine-rich single-stranded DNA and RNA oligonucleotides. *J. Biol. Chem. 277*, 8906−8911.
61. Osborne, S. E., and Ellington, A. D. (1997) Nucleic acids selection and the challenge of combinatorial chemistry. *Chem. Rev. 97*, 349−370.
62. Harada, K., and Frankel, A. D. (1995) Identification of a novel arginine binding DNAs. *EMBO J. 14*, 5798−5811.

BI035754F